Electron Transfer Mechanisms

Deutsche Ausgabe: DOI: 10.1002/ange.201600287
Internationale Ausgabe: DOI: 10.1002/anie.201600287

Enhanced Electron Transfer Reactivity of a Nonheme Iron(IV)–Imido Complex as Compared to the Iron(IV)-Oxo Analogue

Anil Kumar Vardhaman, Yong-Min Lee, Jieun Jung, Kei Ohkubo, Wonwoo Nam, and Shunichi Fukuzumi**

Abstract: *Reactions of N,N-dimethylaniline (DMA) with nonheme iron(IV)-oxo and iron(IV)-tosylimido complexes occur via different mechanisms, such as an N-demethylation of DMA by a nonheme iron(IV)-oxo complex or an electron transfer dimerization of DMA by a nonheme iron(IV)-tosylimido complex. The change in the reaction mechanism results from the greatly enhanced electron transfer reactivity of the iron(IV)-tosylimido complex, such as the much more positive one-electron reduction potential and the smaller reorganization energy during electron transfer, as compared to the electron transfer properties of the corresponding iron-(IV)-oxo complex.*

High-valent metal-oxo and metal-imido complexes have been postulated as active oxidants in oxygen atom and NR group transfer reactions, respectively, by metalloenzymes and bioinspired metal catalysts.[1–3] While extensive studies have been conducted on the reactivities of high-valent metal-oxo complexes over the past several decades,[1,2] much less is known about the reactivities of metal-imido complexes.[2,3] In particular, the chemistry of nonheme iron(IV)-oxo complexes has been well advanced recently by synthesizing a number of biomimetic nonheme iron(IV)-oxo complexes and investigating their reactivities in various oxidation reactions,[1,2] including oxidative N-dealkylation of *N,N*-dimethylanilines (DMA), as well as electrochemical properties (Scheme 1 A).[4] In contrast, only a small number of nonheme iron(IV)-imido complexes have been synthesized, and their chemical properties have been explored less clearly.[5–8] Very recently, an elegant reactivity comparison of nonheme iron-(IV)-oxo versus iron(IV)-imido complexes bearing a common supporting ligand, $[(N4Py)Fe^{IV}(O)]^{2+}$ and $[(N4Py)Fe^{IV}(NTs)]^{2+}$ [N4Py = *N,N*-bis(2-pyridylmethyl)-*N*-bis(2-pyridyl)-methylamine], was reported.[9,10] A contrasting reactivity pattern of the iron(IV)-oxo versus iron(IV)-imido complexes was observed in oxygen atom transfer (OAT) and hydrogen atom transfer (HAT) reactions.[9,10] However, fundamental electron-transfer (ET) properties of nonheme iron(IV)-imido complexes, such as the one-electron reduction potential and the reorganization energy in ET reaction, have never been reported previously. Moreover, the change of reaction mechanism(s) in oxidation reactions by iron(IV)-oxo and iron(IV)-imido complexes has never been demonstrated previously.

A. N-demethylation of *N,N*-dimethylaniline by $[(N4Py)Fe^{IV}(O)]^{2+}$

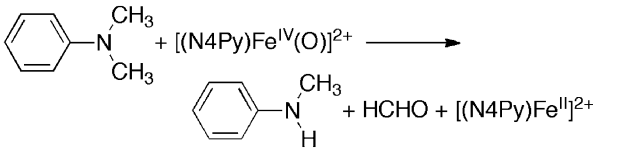

B. Dimerization of *N,N*-dimethylaniline by $[(N4Py)Fe^{IV}(NTs)]^{2+}$

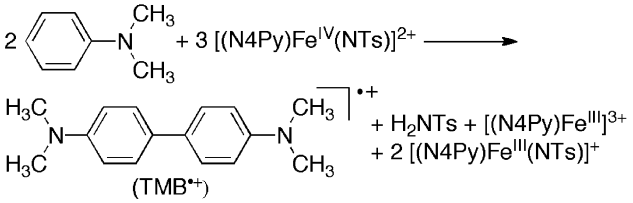

Scheme 1. Reactions of *N,N*-dimethylaniline by A) nonheme iron(IV)-oxo and B) iron(IV)-imido complexes.

Herein, we report that the reactions of DMA with nonheme iron(IV)-oxo and iron(IV)-tosylimido complexes bearing the same supporting ligand, $[(N4Py)Fe^{IV}(O)]^{2+}$ (**1**) and $[(N4Py)Fe^{IV}(NTs)]^{2+}$ (**2**), occur via quite different mechanisms, such as the N-demethylation of DMA by **1** (Scheme 1 A) and the ET dimerization of DMA by **2** (Scheme 1 B). The drastic change of the reaction mechanism from the N-demethylation of DMA by **1** to the ET dimerization of DMA by **2** results from the enhanced electron transfer reactivity of the iron(IV)-tosylimido complex (**2**), such as the more positive one-electron reduction potential and the smaller reorganization energy in electron transfer, as compared to the electron transfer properties of the iron(IV)-oxo analogue (**1**).

Oxidation of DMA by **1** is known to result in the demethylation of DMA (Scheme 1 A).[4] Interestingly, when

[*] Dr. A. K. Vardhaman, Dr. Y.-M. Lee, Dr. J. Jung, Dr. K. Ohkubo, Prof. Dr. W. Nam, Prof. Dr. S. Fukuzumi
Department of Chemistry and Nano Science
Ewha Womans University
Seoul 03760 (Korea)
E-mail: wwnam@ewha.ac.kr
Dr. K. Ohkubo, Prof. Dr. S. Fukuzumi
Faculty of Science and Engineering, ALCA, SENTAN
Japan Science and Technology Agency (JST)
Meijo University
Nagoya, Aichi 468-0073 (Japan)
Dr. K. Ohkubo
Department of Material and Life Science
Graduate School of Engineering, ALCA, SENTAN
Japan Science and Technology Agency (JST)
Osaka University
Suita, Osaka 565-0871 (Japan)

Supporting information for this article can be found under http://dx.doi.org/10.1002/anie.201600287.

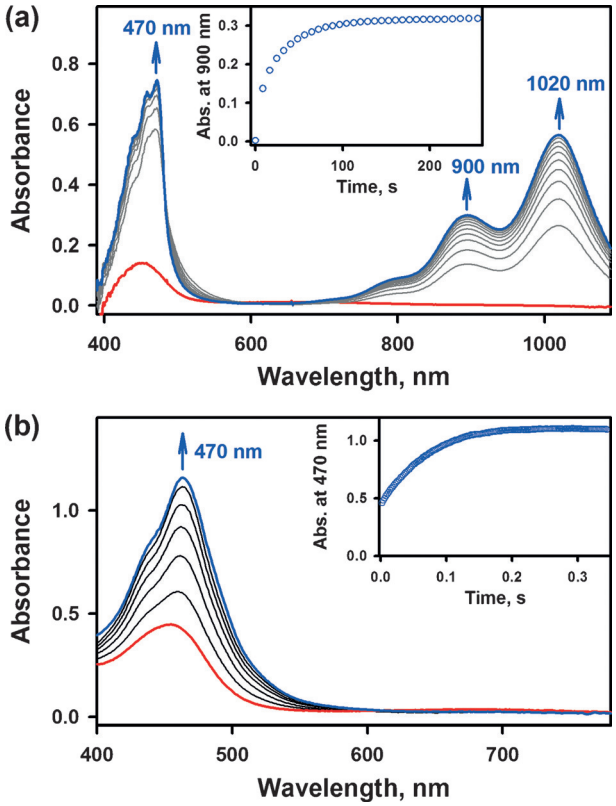

Figure 1. a) Vis-NIR absorption spectral changes in the reaction of $[(N4Py)Fe^{IV}(NTs)]^{2+}$ (5.0×10^{-2} mM) with *N*,*N*-dimethylaniline (5.0×10^{-1} mM) in CH_3CN at 298 K. Inset shows the time course monitored by absorbance change at 900 nm for the formation of $TMB^{\bullet+}$. b) Absorption spectral changes for the formation of $DMA^{\bullet+}$ observed in the reaction of $[(N4Py)Fe^{IV}(NTs)]^{2+}$ (0.125 mM) with DMA (5 equiv, 0.625 mM) in CH_3CN at 298 K. Inset shows the time course monitored by absorbance change at 470 nm for the formation of $DMA^{\bullet+}$.

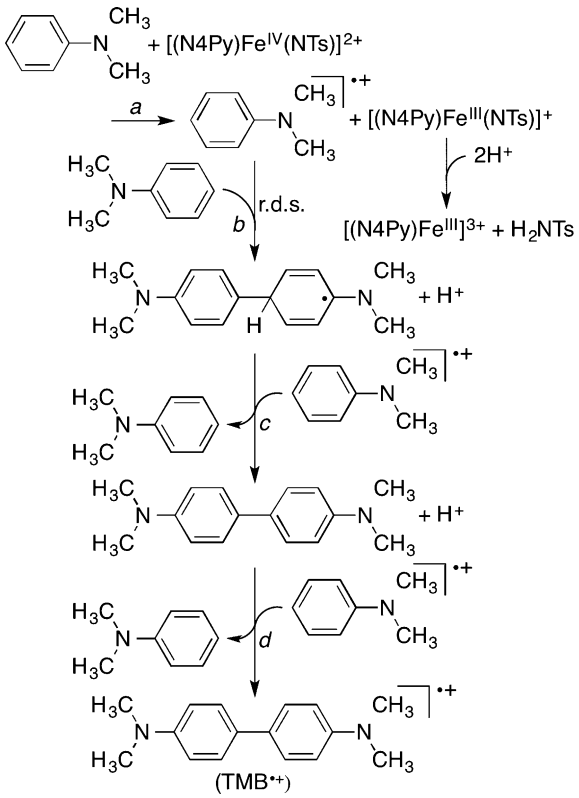

Scheme 2. Proposed mechanism for the dimerization of *N*,*N*-dimethylaniline by $[(N4Py)Fe^{IV}(NTs)]^{2+}$.

1 was replaced by **2**, the oxidized product of DMA was changed from the demethylated product (Scheme 1 A) to a dimer radial cation (tetramethylbenzidine radical cation ($TMB^{\bullet+}$); Scheme 1 B). The quantitative formation of $TMB^{\bullet+}$ in the reaction of DMA with **2** is shown in Figure 1 a, where the absorption bands at 470, 900, and 1020 nm result from the formation of $TMB^{\bullet+}$.[4b,11] The 2:3 stoichiometry for the reaction of DMA with **2** (Scheme 2 B) was established by the absorption spectral titration (Supporting Information, Figure S1). When the products formed in this reaction were analyzed using EPR, two Fe^{III} species with a high-spin ($S=5/2$) state and a low-spin ($S=1/2$) state, along with $TMB^{\bullet+}$, were observed (Figure S2). The Fe^{III} species were assigned as $[(N4Py)Fe^{III}(NTs)]^{+}$ and $[(N4Py)Fe^{III}]^{3+}$. In addition, the ratio of spin amounts of the Fe^{III} species and $TMB^{\bullet+}$ was determined to be 3:1 by the comparison of the doubly integrated values of the EPR signals (Figure S3). The formation of H_2NTs in Scheme 1 B was also confirmed by the ^1H NMR spectrum (Figure S4). $TMB^{\bullet+}$ was formed by the oxidative dimerization of $DMA^{\bullet+}$ ($\lambda_{max}=470$ nm),[11] which was formed by electron transfer from DMA to $[(N4Py)Fe^{IV}(NTs)]^{2+}$ (Figure 1 b; Scheme 2, reaction pathway a). Then, the absorption band at 470 nm from $DMA^{\bullet+}$ was changed to those at 470, 900, and 1020 nm bands owing to $TMB^{\bullet+}$ (Figure 1 a; see below).[4b]

Because the formation of $DMA^{\bullet+}$ was immediate upon addition of DMA to a CH_3CN solution of **2**, the reaction was followed using a stopped-flow spectrophotometer, and by monitoring an increase in the absorption band at 470 nm owing to $DMA^{\bullet+}$ (Figure 1 b, inset; see also Figure S5 for comparison with the formation of $TMB^{\bullet+}$). We also determined the second-order rate constant of $1.4\times10^5\,M^{-1}s^{-1}$ for the formation of $DMA^{\bullet+}$ (Figure S6). When DMA was replaced by a deuterated compound (DMA-$(CD_3)_2$ = *N*,*N*-bis(trideuteriomethyl)aniline), no deuterium kinetic isotope effect (KIE = 1.0(1)) was observed, suggesting that the first step of the formation of $DMA^{\bullet+}$ in the reaction of **2** and DMA occurs via an ET mechanism (Figure S6).

The formation of $TMB^{\bullet+}$ was then monitored by an increase in absorbance at 900 nm, and found to obey first-order kinetics (Figure 1 a, inset). The pseudo-first-order rate constant (k_1) was proportional to the DMA concentration, affording the second-order rate constant (k_{et}) of $1.0(1)\times10^2\,M^{-1}s^{-1}$ (Figure S7). When DMA was replaced by DMA-$(CD_3)_2$, no deuterium kinetic isotope effect was observed (KIE = 1.0(1); Figure S7). This observation is in sharp contrast to the reaction of **1** and DMA, which exhibited a significant kinetic isotope effect owing to a hydrogen atom transfer from the methyl group of DMA to **1**.[4a,c] Furthermore, the formation of $TMB^{\bullet+}$ in the reaction of DMA with **2** was dependent on the DMA concentration (Figure S1), indicating that the rate-determining step is the

C–C bond formation between $DMA^{\bullet+}$ and DMA (Scheme 2, reaction pathway b).

Based on the experimental results described above, we propose the overall mechanism of the DMA oxidation by **2** (Scheme 2). First, electron transfer from DMA to **2** produces $DMA^{\bullet+}$ and $[(N4Py)Fe^{III}(NTs)]^{+}$ (reaction pathway a), followed by the rate-determining C–C bond formation step between $DMA^{\bullet+}$ and DMA to produce a coupling radical product and a proton (reaction pathway b). The coupling radical product is rapidly oxidized by $DMA^{\bullet+}$ to produce TMB and a proton (reaction pathway c). TMB is also readily oxidized by $DMA^{\bullet+}$ to produce $TMB^{\bullet+}$ (reaction pathway d), since the E_{ox} value of TMB (0.32 V vs. SCE)[11] is much lower than that of DMA (0.73 V vs. SCE).[12] Therefore, the overall stoichiometry agrees well with that shown in Scheme 1B. Similarly, the dimerization of triphenylamine (TPA) was observed in the electron transfer oxidation of TPA by **2** to produce a TPA dimer radical cation (Figure S8), with the rate-determining step of the dimerization with TPA (Figure S9).

Then, the one-electron reduction potential of **2** was determined from the electron transfer equilibrium between tris(4-bromophenyl)amine (TBPA) ($E_{ox} = 1.08$ V vs. SCE)[12] and **2**. While no electron transfer from TBPA to **1** ($E_{red} = 0.51$ V vs. SCE)[13] occurs in CH_3CN at 298 K, efficient electron transfer occurs from TBPA to **2** under the same reaction conditions (Figure 2a), where the absorption band at

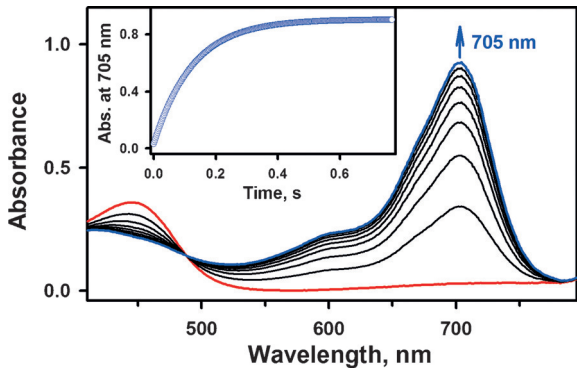

Figure 2. Absorption spectral change for the formation of tris(4-bromophenyl)amine radical cation ($TBPA^{\bullet+}$) produced in electron transfer from TBPA (10 mM) to $[(N4Py)Fe^{IV}(NTs)]^{2+}$ (0.125 mM) in CH_3CN at 298 K. Inset shows the time course monitored by absorbance change at 705 nm.

705 nm is assigned to $TBPA^{\bullet+}$.[14] This result indicates that **2** is a stronger electron acceptor than the corresponding Fe^{IV}-oxo complex, **1**. The electron transfer from TBPA to **2** was found to be in equilibrium, where the final concentration of $TBPA^{\bullet+}$ produced increased with increasing initial concentrations of TBPA to reach a constant value (Figure S10). The equilibrium constant (K_{et}) was determined to be 0.24 at 298 K (see the Supporting Information, Experimental Section and Figure S11). Then, the one-electron reduction potential (E_{red}) of **2** was determined to be 1.04 ± 0.02 V vs. SCE from the K_{et} value and the E_{ox} value of TBPA (1.08 V vs. SCE) using the Nernst equation [Eq. (1)], which is much more positive than the reported value of **1** ($E_{red} = 0.51$ V vs. SCE).[13]

$$E_{red} = E_{ox} + (RT/F)\ln K_{et} \quad (1)$$

The E_{red} value of **2** was confirmed by cyclic voltammetry (Figure S12), showing that the one-electron reduction process of **2** was reversible with the E_{red} value of 1.02 ± 0.02 V (vs. SCE), which agrees well with the value determined by the redox titration (1.04 ± 0.02 V vs. SCE). The large difference in the E_{red} values between **1** and **2** results in the drastic change in the mechanisms of the reactions of DMA with **1** and **2**, because the E_{ox} value of DMA (0.73 V vs. SCE) is higher than the E_{red} value of **1** (0.51 V vs. SCE)[13] but lower than the E_{red} value of **2** (1.04 ± 0.02 V vs. SCE). In such a case, electron transfer from DMA to **1** is highly exergonic when hydrogen atom transfer rather than electron transfer occurs for the N-demethylation (Scheme 1A), whereas electron transfer from DMA to **2** occurs for the formation of $TMB^{\bullet+}$ (Scheme 1B and Scheme 2).

Rates of electron transfer from TBPA to **2** were determined from the rise in the absorption band at 705 nm due to $TBPA^{\bullet+}$ (Figure 2). The electron transfer rates obeyed pseudo-first-order kinetics in the presence of a large excess of TBPA (Figure 2, inset). The pseudo-first-order rate constants (k_{obs}) increased linearly with increasing concentration of TBPA (Figure S13), and the second-order rate constant of the electron transfer (k_{et}) was determined from the slope of the linear plot of k_{obs} versus concentration of TBPA to be $8.5 \times 10^2\,M^{-1}s^{-1}$. Similarly, the k_{et} values of electron transfer from a series of arylamine derivatives to **2** were determined, and the k_{et} values are listed in Table S1 (see also Figure S13), together with the E_{ox} values of arylamine derivatives and the driving force of electron transfer, which was determined using [Eq. (2)], where e is the elementary charge.

$$-\Delta G_{et}\,(eV) = e(E_{red} - E_{ox}) \quad (2)$$

The driving force dependence of the electron transfer rate constants is shown in Figure 3, where the $\log k_{et}$ values are plotted against the $-\Delta G_{et}$ values. The driving force dependence of k_{et} is well fitted by the solid line in Figure 3, in light of the Marcus theory of adiabatic outer-sphere electron transfer [Eq. (3)],

$$k_{et} = Z\exp[-(\lambda/4)(1 + \Delta G_{et}/\lambda)^2/k_B T] \quad (3)$$

where Z is the collision frequency taken as $1 \times 10^{11}\,M^{-1}s^{-1}$, λ is the reorganization energy of electron transfer, k_B is the Boltzmann constant, and T is the absolute temperature.[15,16] The λ value is determined to be 1.89 eV as the best fit value of [Eq. (3)], and this value is significantly smaller than that of **1** (2.74 eV).[13] The $\log k_{et}$ value of the reactions of DMA with **2** (number 5 in Figure 3) agrees with the Marcus line with $\lambda = 1.89$ eV for the electron transfer from arylamine derivatives to **2**.

The higher E_{red} value of **2** than that of **1** was supported by the density functional theory (DFT) calculations at the CAM-B3LYP/6-311G(d) level of theory (Supporting Information),[17,18] which shows that the LUMO level of **2** ($S = 1$) was 0.4 eV lower than that of **1** ($S = 1$; Figure S14). The bond reorganization energies of electron transfer (λ_i) of

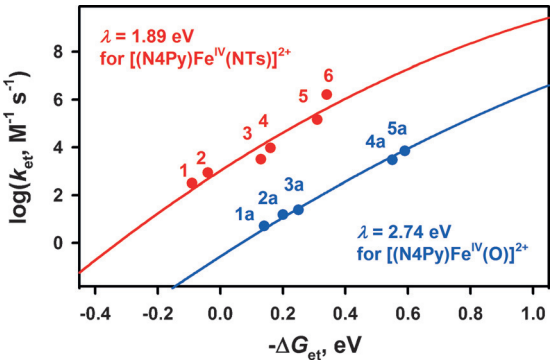

Figure 3. a) Plots of logk_{et} of electron transfer from arylamines [1: 4-CN-DMA; 2: (4-Br-C_6H_4)$_3$N (=TBPA); 3: (C_6H_5)$_3$N (=TPA); 4: 4-Br-DMA; 5: DMA; and 6: 4-Me-DMA] to [(N4Py)Fe^{IV}(NTs)]$^{2+}$ (red circles) in CH_3CN at 298 K vs. the driving force of the electron transfer. b) Plots of logk_{et} of electron transfer from ferrocene derivatives [1a: ferrocene; 2a: *n*-amyl ferrocene; 3a: dimethylferrocene; 4a: octamethylferrocene; and 5a: decamethylferrocene] to [(N4Py)Fe^{IV}(O)]$^{2+}$ (blue circles) in CH_3CN at 298 K vs. the driving force of the electron transfer.[13] The fitting to the Marcus theory of the electron transfer are shown by the red line with $\lambda = 1.89$ eV and blue line with $\lambda = 2.74$ eV.

2/[(N4Py)Fe^{III}(NTs)]$^+$ and **1**/[(N4Py)Fe^{III}(O)]$^+$ were also evaluated by using the density DFT calculations.[19] The λ_i value of **2**/[(N4Py)Fe^{III}(NTs)]$^+$ was estimated to be 0.72 eV as an energy difference between the optimized structure of **2** ($S=1$) and the optimized structure of [(N4Py)Fe^{III}(NTs)]$^+$ ($S=1/2$; Figure S15). This value is 1.58 eV smaller than the corresponding λ_i value of **1** ($S=1$)/[(N4Py)Fe^{III}(O)]$^+$ ($S=1/2$).[20] The difference in the λ value (0.85 eV) observed in the one-electron reduction processes of **2** ($\lambda = 1.89$ eV) and **1** ($\lambda = 2.74$ eV) corresponds to about one-half of the difference in the λ_i values (1.58 eV) of electron exchanges of **2** ($S=1$)/[(N4Py)Fe^{III}(NTs)]$^+$ ($S=1/2$) and **1** ($S=1$)/[(N4Py)Fe^{III}(O)]$^+$ ($S=1/2$; Table S2). The smaller λ value of **2** than that of **1** may result due to the smaller change in the bond lengths by the ET reduction of **2**.

In conclusion, we have shown that a nonheme iron(IV)-tosylimido complex, [(N4Py)Fe^{IV}(NTs)]$^{2+}$ (**2**), acts as a much stronger electron acceptor than the corresponding iron(IV)-oxo complex, [(N4Py)Fe^{IV}(O)]$^{2+}$ (**1**), but a one-electron reduced complex, [(N4Py)Fe^{III}(NTs)]$^+$, acts as a much weaker base than the corresponding iron(III)-oxo complex, [(N4Py)Fe^{III}(O)]$^+$. Such differences in the redox and acid–base properties resulted in the drastic change in the reaction mechanisms from the N-demethylation of DMA by [(N4Py)Fe^{IV}(O)]$^{2+}$ (**1**) via hydrogen atom transfer to the electron transfer dimerization of DMA by [(N4Py)Fe^{IV}-(NTs)]$^{2+}$ (**2**) to form TMB$^{\bullet+}$ product.

Acknowledgements

This work was supported by the NRF of Korea through CRI (NRF-2012R1A3A2048842 to W.N.), GRL (NRF-2010-00353 to W.N.) and ALCA and SENTAN projects from JST, Japan (to S.F.) and JSPS (26620154 and 26288037) from MEXT (to K.O.).

Keywords: bioinorganic chemistry · electron transfer · iron(IV)-imido complexes · mechanisms · N-demethylation

How to cite: *Angew. Chem. Int. Ed.* **2016**, *55*, 3709–3713
Angew. Chem. **2016**, *128*, 3773–3777

[1] a) S. L.-F. Chan, Y.-H. Kan, K.-L. Yip, J.-S. Huang, C.-M. Che, *Coord. Chem. Rev.* **2011**, *255*, 899; b) G. Yin, *Acc. Chem. Res.* **2013**, *46*, 483; c) M. Costas, *Coord. Chem. Rev.* **2011**, *255*, 2912; d) S. P. de Visser, J.-U. Rohde, Y.-M. Lee, J. Cho, W. Nam, *Coord. Chem. Rev.* **2013**, *257*, 381; e) K. Ray, F. F. Pfaff, B. Wang, W. Nam, *J. Am. Chem. Soc.* **2014**, *136*, 13942; f) W. Nam, Y.-M. Lee, S. Fukuzumi, *Acc. Chem. Res.* **2014**, *47*, 1146; g) S. Fukuzumi, *Dalton Trans.* **2015**, *44*, 6696; h) S. A. Cook, A. S. Borovik, *Acc. Chem. Res.* **2015**, *48*, 2407; i) W. N. Oloo, L. Que, Jr., *Acc. Chem. Res.* **2015**, *48*, 2612; j) H. M. Neu, R. A. Bagila, D. P. Goldberg, *Acc. Chem. Res.* **2015**, *48*, 2754.

[2] a) K. Ray, F. Heims, F. F. Pfaff, *Eur. J. Inorg. Chem.* **2013**, 3784; b) H.-Y. Liua, M. H. Mahmood, S.-X. Qiu, C. K. Chang, *Coord. Chem. Rev.* **2013**, *257*, 1306; c) J. M. Smith, D. Subedi, *Dalton Trans.* **2012**, *41*, 1423; d) J. Hohenberger, K. Ray, K. Meyer, *Nat. Commun.* **2012**, *3*, 720; e) C.-M. Che, V. K.-Y. Lo, C.-Y. Zhou, J.-S. Huang, *Chem. Soc. Rev.* **2011**, *40*, 1950; f) G. Du, M. M. Abu-Omar, *Curr. Org. Chem.* **2008**, *12*, 1185; g) D. P. Goldberg, *Acc. Chem. Res.* **2007**, *40*, 626.

[3] a) W.-L. Man, W. W. Y. Lam, T.-C. Lau, *Acc. Chem. Res.* **2014**, *47*, 427; b) M. M. Abu-Omar, *Dalton Trans.* **2011**, *40*, 3435; c) C.-M. Che, C.-Y. Zhou, E. L.-M. Wong, *Top. Organomet. Chem.* **2011**, *33*, 111; d) M. P. Mehn, J. C. Peters, *J. Inorg. Biochem.* **2006**, *100*, 634.

[4] a) K. Nehru, M. S. Seo, J. Kim, W. Nam, *Inorg. Chem.* **2007**, *46*, 293; b) J. Park, Y. Morimoto, Y.-M. Lee, Y. You, W. Nam, S. Fukuzumi, *Inorg. Chem.* **2011**, *50*, 11612; c) A. Barbieri, M. De Gennaro, S. Di Stefano, O. Lanzalunga, A. Lapi, M. Mazzonna, G. Olivo, B. Ticconi, *Chem. Commun.* **2015**, *51*, 5032.

[5] a) M. J. Zdilla, M. M. Abu-Omar, *J. Am. Chem. Soc.* **2006**, *128*, 16971; b) M. J. Zdilla, J. L. Dexheimer, M. M. Abu-Omar, *J. Am. Chem. Soc.* **2007**, *129*, 11505; c) M. J. Zdilla, M. M. Abu-Omar, *Inorg. Chem.* **2008**, *47*, 10722; d) P. Leeladee, G. N. L. Jameson, M. A. Siegler, D. Kumar, S. P. de Visser, D. P. Goldberg, *Inorg. Chem.* **2013**, *52*, 4668.

[6] a) W.-L. Man, W. W. Y. Lam, H.-K. Kwong, T.-C. Lau, *Angew. Chem. Int. Ed.* **2012**, *51*, 9101; *Angew. Chem.* **2012**, *124*, 9235; b) W.-L. Man, J. Xie, Y. Pan, W. W. Y. Lam, H.-K. Kwong, K.-W. Ip, T.-C. Lau, *J. Am. Chem. Soc.* **2013**, *135*, 5533; c) Y. Liu, X. Guan, E. L.-M. Wong, P. Liu, J.-S. Huang, C.-M. Che, *J. Am. Chem. Soc.* **2013**, *135*, 7194.

[7] a) L. Wang, L. Hu, H. Zhang, H. Chen, L. Deng, *J. Am. Chem. Soc.* **2015**, *137*, 14196; b) L. Zhang, Y. Liu, L. Deng, *J. Am. Chem. Soc.* **2014**, *136*, 15525; c) K. Searles, S. Fortier, M. M. Khusniyarov, P. J. Carroll, J. Sutter, K. Meyer, D. J. Mindiola, K. G. Caulton, *Angew. Chem. Int. Ed.* **2014**, *53*, 14139; *Angew. Chem.* **2014**, *126*, 14363.

[8] a) E. Gouré, F. Avenier, P. Dubourdeaux, O. Sénèque, F. Albrieux, C. Lebrun, M. Clémancey, P. Maldivi, J.-M. Latour, *Angew. Chem. Int. Ed.* **2014**, *53*, 1580; *Angew. Chem.* **2014**, *126*, 1606; b) I. Nieto, F. Ding, R. P. Bontchev, H. Wang, J. M. Smith, *J. Am. Chem. Soc.* **2008**, *130*, 2716; c) C. M. Thomas, N. P. Mankad, J. C. Peters, *J. Am. Chem. Soc.* **2006**, *128*, 4956; d) S. C. Bart, E. Lobkovsky, E. Bill, P. J. Chirik, *J. Am. Chem. Soc.* **2006**, *128*, 5302; e) R. L. Lucas, D. R. Powell, A. S. Borovik, *J. Am. Chem. Soc.* **2005**, *127*, 11596.

[9] E. J. Klinker, T. A. Jackson, M. P. Jensen, A. Stubna, G. Juhász, E. L. Bominaar, E. Münck, L. Que, Jr., *Angew. Chem. Int. Ed.* **2006**, *45*, 7394; *Angew. Chem.* **2006**, *118*, 7554.

[10] a) A. K. Vardhaman, P. Barman, S. Kumar, C. V. Sastri, D. Kumar, S. P. de Visser, *Angew. Chem. Int. Ed.* **2013**, *52*, 12288;

Angew. Chem. **2013**, *125*, 12514; b) S. Kumar, A. S. Faponle, P. Barman, A. K. Vardhaman, C. V. Sastri, D. Kumar, S. P. de Visser, *J. Am. Chem. Soc.* **2014**, *136*, 17102.
[11] M. Kirchgessner, K. Sreenath, K. R. Gopidas, *J. Org. Chem.* **2006**, *71*, 9849.
[12] The oxidation potentials of DMA and TPA derivatives were determined by cyclic voltammetry (CV), differential pulse voltammetry (DPV), and second harmonic alternative current voltammetry (SHACV) in CH_3CN at 298 K (Table S1).
[13] Y.-M. Lee, H. Kotani, T. Suenobu, W. Nam, S. Fukuzumi, *J. Am. Chem. Soc.* **2008**, *130*, 434.
[14] a) M. Oyama, T. Higuchi, *J. Electrochem. Soc.* **2002**, *149*, E12; b) S. Amthor, B. Noller, C. Lambert, *Chem. Phys.* **2005**, *316*, 141.
[15] S. Fukuzumi, *Coord. Chem. Rev.* **2013**, *257*, 1564.
[16] a) R. A. Marcus, *Annu. Rev. Phys. Chem.* **1964**, *15*, 155; b) R. A. Marcus, *Angew. Chem. Int. Ed. Engl.* **1993**, *32*, 1111; *Angew. Chem.* **1993**, *105*, 1161.
[17] M. J. Frisch et al., Gaussian 09, revision A.02; Gaussian, Inc.: Wallingford, CT, **2009** (Full author list is shown in the Supporting Information).
[18] A. D. Becke, *J. Chem. Phys.* **1993**, *98*, 5648.
[19] C. Lee, W. Yang, R. G. Parr, *Phys. Rev. B* **1988**, *37*, 785.
[20] Because electron transfer from electron donors ($S=0$) to the Fe^{IV} complexes ($S=1$; overall spin = 1) to produce donor radical cations ($S=1/2$) and the Fe^{III} complexes ($S=5/2$; overall spin = 2 or 3) is spin forbidden, the low spin state of the Fe^{III} complexes ($S=1/2$) was used for the calculations; see also Y. Kawashima, K. Ohkubo, S. Fukuzumi, *J. Phys. Chem. A* **2013**, *117*, 6737.

Received: January 11, 2016
Revised: January 26, 2016
Published online: February 17, 2016

